

A CROSSED MOLECULAR BEAM, LOW-TEMPERATURE KINETICS, AND THEORETICAL INVESTIGATION OF THE REACTION OF THE CYANO RADICAL (CN) WITH 1,3-BUTADIENE (C₄H₆). A ROUTE TO COMPLEX NITROGEN-BEARING MOLECULES IN LOW-TEMPERATURE EXTRATERRESTRIAL ENVIRONMENTS

SÉBASTIEN B. MORALES^{1,5}, CHRISTOPHER J. BENNETT^{1,5,6}, SÉBASTIEN D. LE PICARD^{1,7}, ANDRÉ CANOSA¹, IAN R. SIMS^{1,7}, B. J. SUN², P. H. CHEN², AGNES H. H. CHANG^{2,7}, VADIM V. KISLOV³, ALEXANDER M. MEBEL^{3,7}, XIBIN GU⁴, FANGTONG ZHANG⁴, PAVLO MAKSYUTENKO⁴, AND RALF I. KAISER^{4,7}

¹ Institut de Physique de Rennes, Equipe Astrochimie Expérimentale, UMR UR1-CNRS 6251,

Université de Rennes 1, Campus de Beaulieu 35042 Rennes Cedex, France; sebastien.le-picard@univ-rennes1.fr, ian.sims@univ-rennes1.fr

² Department of Chemistry, National Dong Hwa University, Hualien, Taiwan; hhchang@mail.ndhu.edu.tw

³ Department of Chemistry and Biochemistry, Florida International University, Miami, FL, USA; mebela@fiu.edu

⁴ Department of Chemistry, University of Hawaii at Manoa, Honolulu, HI, USA; ralfk@hawaii.edu

Received 2011 June 2; accepted 2011 August 25; published 2011 November 2

ABSTRACT

We present a joint crossed molecular beam and kinetics investigation combined with electronic structure and statistical calculations on the reaction of the ground-state cyano radical, CN($X^2\Sigma^+$), with the 1,3-butadiene molecule, H₂CCHCHCH₂(X^1A_g), and its partially deuterated counterparts, H₂CCDCDCH₂(X^1A_g) and D₂CCHCHCD₂(X^1A_g). The crossed beam studies indicate that the reaction proceeds via a long-lived C₅H₆N complex, yielding C₅H₅N isomer(s) plus atomic hydrogen under single collision conditions as the nascent product(s). Experiments with the partially deuterated 1,3-butadienes indicate that the atomic hydrogen loss originates from one of the terminal carbon atoms of 1,3-butadiene. A combination of the experimental data with electronic structure calculations suggests that the thermodynamically less favorable 1-cyano-1,3-butadiene isomer represents the dominant reaction product; possible minor contributions of less than a few percent from the aromatic pyridine molecule might be feasible. Low-temperature kinetics studies demonstrate that the overall reaction is very fast from room temperature down to 23 K with rate coefficients close to the gas kinetic limit. This finding, combined with theoretical calculations, indicates that the reaction proceeds on an entrance barrier-less potential energy surface (PES). This combined experimental and theoretical approach represents an important step toward a systematic understanding of the formation of complex, nitrogen-bearing molecules—here on the C₅H₆N PES—in low-temperature extraterrestrial environments. These results are compared to the reaction dynamics of D1-ethynyl radicals (C₂D; $X^2\Sigma^+$) with 1,3-butadiene accessing the isoelectronic C₆H₇ surface as tackled earlier in our laboratories.

Key words: astrochemistry – methods: laboratory – molecular processes

Online-only material: color figures

1. INTRODUCTION

More than 160 molecules have been detected in the interstellar medium (ISM) or in circumstellar envelopes among which more than 25% contain both carbon and nitrogen atoms, which are respectively, the fourth and sixth most abundant elements in the universe. In recent years, particular efforts have been made to probe the limits of molecular complexity in diffuse (Liszt et al. 2008) and dense clouds (Belloche et al. 2009). Detection of large species is rather challenging work as complex molecules usually have large partition functions and consequently weak individual lines. Recently, for instance, *n*-propyl cyanide (C₃H₇CN; Belloche et al. 2009), amino acetonitrile (NH₂CH₂CN; Belloche et al. 2008), methylcyanodiacetylene (CH₃C₅N; Snyder et al. 2006), cyanoallene (CH₂CCHCN; Chin et al. 2006; Lovas et al. 2006b), and ketenimine (CH₂CNH; Lovas et al. 2006a) have been detected in Sagittarius B2(N) hot cores or in the Taurus Molecular Cloud 1. Such interstellar detections can also serve as indicators of gas-phase production schemes because they can help establish the role of functional groups such as CH₃ or CN in

the formation of large interstellar species, though the participation of interstellar grain chemistry is likely also to be of importance especially in young stellar objects (Herbst & van Dishoeck 2009). Additional information can be obtained by detecting isomeric molecules, using, for instance, hyperfine structure identification (Lovas et al. 2006b), as it is expected that gas-phase chemistry may favor the production of one isomer or another, depending on the mechanism involved. Laboratory and theoretical studies can provide complementary information to understand the variation of abundances observed in different objects of the ISM that will depend on physical conditions. While the most complex molecule identified so far in the ISM, HC₁₁N, contains 13 atoms, it is expected that much more complex molecules are present, such as polycyclic aromatic hydrocarbons (PAHs) and related species that are presumed to be responsible for the emission features detected at 3.3, 6.2, 7.7, 8.8, and 11.2 μm, the so-called unidentified infrared (UIR) bands (Peeters 2011).

PAHs, including (de)hydrogenated and ionized species, as well as nitrogen substituted PAHs are among the most fascinating molecules thought to exist in the ISM (Rhee et al. 2007). The postulation of their interstellar relevance as the missing link between small carbon clusters and amorphous carbon particles fueled enormous scientific effort (Cook et al. 1996). Today, PAH-like species, which are presumed to contain up to 30% of the cosmic carbon (Allamandola et al. 1989; Draine & Li 2007;

⁵ Contributed equally to this work.

⁶ Visiting scientist. Current address: Department of Chemistry, University of Hawaii at Manoa, Honolulu, HI, USA.

⁷ Authors to whom correspondence should be addressed.

Li & Draine 2001; Snow & Witt 1995), have been implicated in the astrobiological evolution of the ISM (Des Marais et al. 2008) and provide nucleation sites for the formation of carbonaceous dust particles. They have also been linked to the UIR emission bands observed in the range of 3–14 μm (3300–700 cm^{-1} ; Allamandola et al. 1985) and to the diffuse interstellar bands (DIBs; Salama & Allamandola 1992), discrete absorption features superimposed on the interstellar extinction curve ranging from the blue part of the visible (400 nm) to the near-infrared (1.2 μm). Although neither individual nor nitrogen-substituted PAHs have been detected in the ISM, their simplest building block—the aromatic benzene molecule (C_6H_6)—was identified with the *Infrared Space Observatory (ISO)* toward the protoplanetary nebula CRL 618 (Cernicharo et al. 2001). Recent laboratory studies under single collision conditions combined with electronic structure calculations and astrochemical modeling have shown that the benzene molecule can be formed via a barrier-less, exoergic reaction of the ethynyl radical (C_2H ; $X^2\Sigma^+$) with 1,3-butadiene at fractions of $30\% \pm 10\%$ via a complex forming reaction mechanism; the thermodynamically less stable hexa-1,3-dien-5-yne isomer was found to be a second isomer synthesized under single collision conditions in the gas phase on the C_6H_7 potential surface (Jones et al. 2011). However, the detection and elucidation of formation routes of the simplest nitrogen-bearing aromatic molecule, pyridine ($\text{C}_5\text{H}_5\text{N}$), which is isoelectronic to the benzene molecule, together with its acyclic isomers, in cold extraterrestrial environments such as in the ISM and in the atmosphere of Saturn’s moon Titan has remained elusive to date and was one of the principal motivations for the present study. Only one study has demonstrated the formation of pyridine in an elementary reaction in the gas phase (Soorkia et al. 2010), though this was a ring expansion reaction ($\text{CH} + \text{pyrrole}$) rather than a direct cyclization.

Since the chemical evolution of low-temperature environments involves multiple elementary reactions that are a series of bimolecular encounters between molecules, radicals, and atoms, a detailed understanding of the underlying mechanisms involved at the most fundamental, microscopic level is crucial. These include experiments under single collision conditions using the crossed molecular beam technique in which *one* particle from a primary reactant beam is made to collide with only *one* particle from the secondary beam. Here, bimolecular gas-phase reactions of ground-state cyano radicals (CN ; $X^2\Sigma^+$) with unsaturated hydrocarbons such as acetylene (C_2H_2), diacetylene (HCCCCH), ethylene (C_2H_4), and benzene (C_6H_6), displayed no entrance barriers to reaction and followed cyano radical versus atomic hydrogen exchange pathways (Kaiser & Balucani 2001). This resulted in the formation of important hydrogen-deficient nitriles, i.e., organic molecules carrying a cyano (CN) group, such as cyanoacetylene (HCCCN), cyanodiacetylene (HCCCCN), and vinyl cyanide ($\text{C}_2\text{H}_3\text{CN}$), which have been detected in the ISM. Previous studies of the reactions of the isoelectronic C_2H and CN radicals with unsaturated hydrocarbons have shown that there is often a strong parallel both in terms of low-temperature reactivity and major products. For example, C_2H and CN show similar reactivity with acetylene (Chastaing et al. 1998; Sims et al. 1993), and form the equivalent isoelectronic products diacetylene (Stahl et al. 2002) and cyanoacetylene (Balucani et al. 2000). Based on these data, it is sensible to envisage that the reaction of cyano radicals with the 1,3-butadiene molecule ($\text{H}_2\text{CCHCHCH}_2$; X^1A_g) should lead to species of the molecular formula $\text{C}_5\text{H}_5\text{N}$ —possibly

the aromatic pyridine molecule together with its acyclic isomer(s)—plus atomic hydrogen. Therefore, we conducted a combined crossed molecular beam and kinetics investigation on the reaction of the ground-state cyano radical (CN ; $X^2\Sigma^+$) with 1,3-butadiene ($\text{H}_2\text{CCHCHCH}_2$; X^1A_g) and merged these experiments with electronic structure and statistical calculations to elucidate the formation of complex nitrogen-bearing molecules, i.e., $\text{C}_5\text{H}_5\text{N}$ isomer(s), under single collision conditions in low-temperature environments and to extract the underlying reaction mechanisms.

2. EXPERIMENTAL

2.1. Crossed Beam Experiments

A pulsed, supersonic beam of ground-state cyano radicals, $\text{CN}(X^2\Sigma^+)$, was generated in situ by focusing about 10 mJ of the fourth harmonic output of an Nd:YAG laser at 266 nm at a repetition rate of 30 Hz onto a rotating graphite rod and seeding the ablated species in molecular nitrogen gas (Gaspro; 99.9999%) at 4 atm backing pressure, which also acted as a reagent gas (Kaiser et al. 1999). A four-slot chopper wheel, located after the skimmer and prior to the interaction region, selected a part of the pulsed cyano radical beam with a peak velocity of $1581 \pm 21 \text{ ms}^{-1}$ and a speed ratio of 2.5 ± 0.1 . The electronic ground state of the cyano radical was probed via laser-induced fluorescence (LIF) through the $B^2\Sigma^+ - X^2\Sigma^+$ (0,0), (1,1), and (2,2) vibrational bands at $\sim 387 \text{ nm}$ by the pulsed 4 μJ output of a Lambda Physik Scanmate dye laser. We observed cyano radicals in the vibrational ground state ($v = 0$; 74%), and in the first and second vibrationally excited states at fractions of 17% and 9%, respectively; for $v = 0$ and 1, bimodal rovibrational distributions characterized by rotational temperatures of 1500 K and 300 K were found. The cyano radical beam segment perpendicularly crossed a pulsed beam of 1,3-butadiene (Fluke; $\geq 99.5\%$) released by a second pulsed valve at a backing pressure of 550 Torr. The section of the 1,3-butadiene beam, interacting with the cyano radical beam, was characterized by a peak velocity of $691 \pm 22 \text{ m s}^{-1}$ and a speed ratio of 6.9 ± 0.7 ; the nominal collision energy was $26.1 \pm 0.9 \text{ kJ mol}^{-1}$. To obtain information on the position of the atomic hydrogen loss, partially deuterated 1,3-butadienes (1,1,4,4-D4–1,3-butadiene and 2,3-D2–1,3-butadiene) were also used in the experiments; however, due to the high costs, data were only collected at the corresponding center-of-mass (CM) angles. A triply differentially pumped quadrupole mass spectrometer coupled to an electron-impact ionizer operated at 2 mA and electron energies of 80 eV recorded time-of-flight (TOF) spectra at various laboratory angles of ions at mass-to-charge from $m/z = 79$ ($\text{C}_5\text{H}_5\text{N}^+$) and lower. We would like to stress that the ablation beam also contains ground-state carbon atoms ($\text{C}(^3P_1)$) as well as dicarbon and tricarbon molecules. However, atomic carbon reacts with 1,3-butadiene only to C_5H_5 products at $m/z = 65$ (Hahndorf et al. 2000) and does not interfere with the signal of $\text{C}_5\text{H}_5\text{N}$ at $m/z = 79$. Tricarbon reactions have significant entrance barriers (Kaiser & Balucani 2001); therefore, tricarbon molecules do not react with 1,3-butadiene under the present experimental conditions. Dicarbon molecules were produced to a fraction of a few percent. This would result only in C_6H_5 products at m/z ratios lower than $m/z = 79$ (Zhang et al. 2010). Therefore, only reactions from cyano radicals contribute to the signal at $m/z = 79$. To collect information on the scattering dynamics, the laboratory data

(TOF, laboratory angular distribution) were transformed into the CM reference frame utilizing a forward-convolution routine (Entenman 1986). This iterative method initially assumes the angular flux distribution, $T(\theta)$, and the translational energy flux distribution, $P(E_T)$ in the CM system. Laboratory TOF spectra and the laboratory angular distributions (LAB) were then calculated from these $T(\theta)$ and $P(E_T)$ functions and were averaged over a grid of Newton diagrams; the fitting program accounts for the apparatus functions and for the spread in the velocity distribution (speed ratio).

2.2. Kinetics Experiments

The kinetics experiments were performed using a continuous flow CRESU apparatus to provide gas mixtures at low temperatures (Sims et al. 1994). In the CRESU technique, low temperatures are achieved through the isentropic supersonic expansion of a buffer gas through an axisymmetric convergent–divergent Laval nozzle. Each Laval nozzle provides an axially and radially uniform supersonic flow at a well-defined temperature, density, and velocity for a given buffer gas. All these properties are conserved in the core of the flow over a length of a few tens of centimeters. The relatively high density of the supersonic flow (typically, 10^{16} – 10^{17} cm^{-3}) ensures that frequent collisions maintain thermal equilibrium. In the present kinetics experiments, seven different Laval nozzles were employed to derive rate coefficients for the reaction between ground-state cyano radicals, $\text{CN}(X^2\Sigma^+)$, and 1,3-butadiene ($\text{H}_2\text{CCHCHCH}_2$; X^1A_g) at temperatures between 23 K and 298 K. To generate cyano radicals, cyanogen iodide (ICN; Aldrich, 95%) was photolyzed at 266 nm using the fourth harmonic of an Nd:YAG laser (Spectra Physics GCR 190) at a fluence in the reaction zone of about 80 mJ cm^{-2} . A small flow of a few $\text{cm}^3 \text{ minute}^{-1}$ of helium was passed over crystals of cyanogen iodide before entering the gas reservoir upstream of the Laval nozzle. The main gases were taken directly from cylinders and regulated by means of separately calibrated Tylan mass flow controllers. The purities of the gases used are given by the manufacturer (Air Liquide) as follows: argon (Ar) $\geq 99.997\%$, helium (He) and nitrogen (N_2) $\geq 99.995\%$, and 1,3-butadiene ($\text{H}_2\text{CCHCHCH}_2$) $> 99.6\%$.

The photodissociation of cyanogen iodide at 266 nm produces cyano radicals that are overwhelmingly in the vibrational ground state ($v = 0$) of the $X^2\Sigma^+$ electronic ground state, but over a wide range of rotational levels (Baronovski & McDonald 1977). Cyano radicals were detected by exciting them in the (0,0) band of the $B^2\Sigma^+ - X^2\Sigma^+$ system at about 388 nm using the doubled idler output of a tunable optical parametric oscillator (Spectra Physics MOPO) pumped by the tripled output of another Nd:YAG laser (Spectra Physics GCR 230). Fluorescence in the (0,1) band at about 420 nm was collected via an appropriate combination of an ultraviolet (UV)-enhanced mirror and fused silica lenses onto the photocathode of a photomultiplier tube (EMI 9124B) through a narrow-band interference filter centered at 420 nm with a 10 nm bandwidth (Ealing Optics). Decay traces, like the one shown in Figure 1, were obtained by recording the integrated LIF intensity as the delay time between the photolysis and probe pulses systematically varied between zero and typically a few hundred microseconds. These traces of the LIF signal versus the time delay were fitted to single exponential decay functions, starting the fit at time delays long enough to allow for rotational relaxation. This procedure yielded pseudo-first-order rate coefficients, k_{1st} , related to the rate of loss of cyano radicals. Second-order rate coefficients, k , were obtained

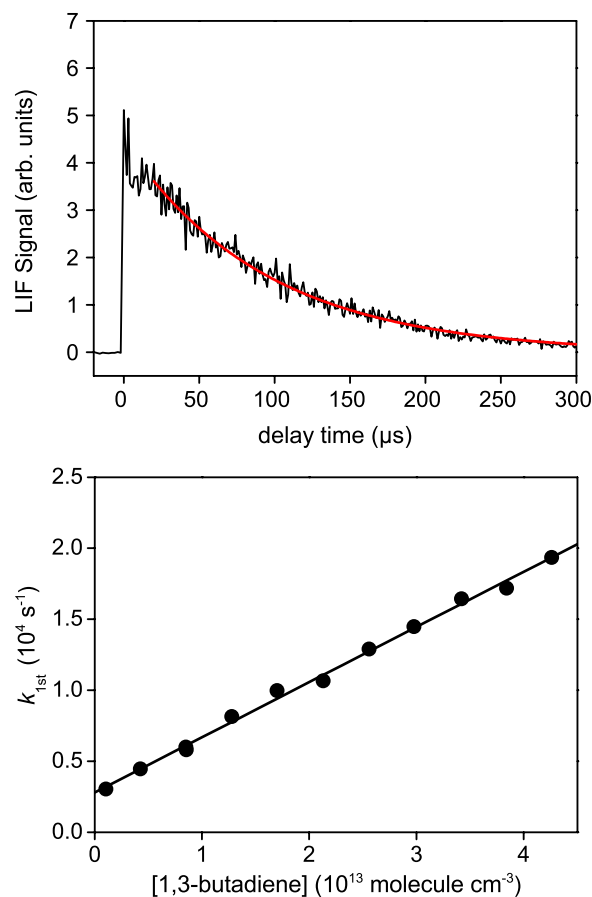


Figure 1. Upper panel: decay of $B^2\Sigma^+ \rightarrow X^2\Sigma^+$ LIF signal from the cyano radical at 52.3 K in the presence of 1,3-butadiene ($[\text{C}_4\text{H}_6] = 2.13 \times 10^{13} \text{ molecule cm}^{-3}$) and argon buffer ($[\text{Ar}] = 1.03 \times 10^{17} \text{ molecule cm}^{-3}$); the data could be fit to a single exponential decay function; lower panel: second-order plot for the reaction of cyano radicals with 1,3-butadiene at 52.3 K in argon leading to a value for the second-order rate coefficient of $k = (3.89 \pm 0.42) \times 10^{-10} \text{ cm}^3 \text{ molecule}^{-1} \text{ s}^{-1}$.

(A color version of this figure is available in the online journal.)

by varying the concentration of 1,3-butadiene, $[\text{C}_4\text{H}_6]$, and then plotting k_{1st} against $[\text{C}_4\text{H}_6]$ as shown in Figure 1 (lower panel).

2.3. Electronic Structure and Statistical Calculations

Electronic structure calculations have been carried out to explore probable low-energy pathways leading to dissociation products for the cyano radical plus 1,3-butadiene reaction on the adiabatic doublet C_5NH_6 PES. The optimized geometries and harmonic frequencies of intermediates, transition states, and dissociation products along the reaction paths are obtained at the level of the hybrid density functional theory, the unrestricted B3LYP/cc-pVTZ (Becke 1993; Lee et al. 1988), and the energies at 0 K are refined with coupled cluster CCSD(T)/cc-pVTZ with B3LYP/cc-pVTZ zero-point energy corrections (Pople et al. 1987; Purvis & Bartlett 1982; Scuseria et al. 1988; Scuseria & Schaefer 1989). For the most important intermediates and transition states, additional CCSD(T)/cc-pVDZ and CCSD(T)/cc-pVQZ calculations were performed and the results were extrapolated to the complete basis set CCSD(T)/CBS limit. The GAUSSIAN 03 and MOLPRO 2006 programs were utilized in the calculations (Frisch et al. 2004; Werner et al. 2006). For these polyatomic systems, the energies of the intermediates, products, and transition states are expected to be accurate within $\pm 8 \text{ kJ mol}^{-1}$ (Peterson

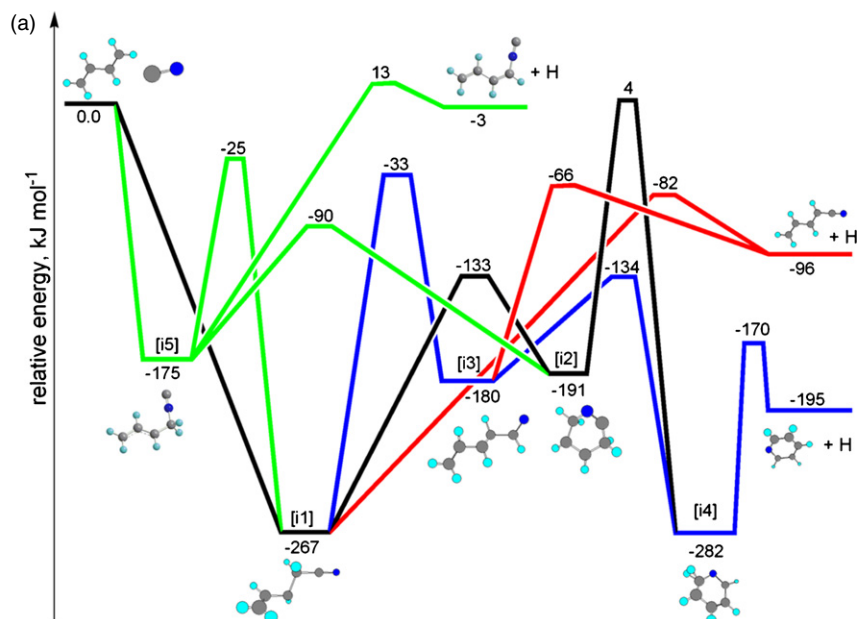


Figure 2. (a) Potential energy surface for the cyano radical plus 1,3-butadiene reaction to form 1-cyano-1,3-butadiene plus atomic hydrogen (blue lines) and pyridine plus atomic hydrogen (red lines). Black balls depict carbon, dark blue balls nitrogen, and light blue balls hydrogen atoms. Green lines: pathways originating from addition of the cyano radical with the nitrogen atom; red lines: pathways to the 1-cyano-1,3-butadiene isomer; blue and black lines: two pathways to intermediate [i4] leading to the pyridine molecule. (b) Geometries of reactant, products, and transition states of those stationary points referred to in panel (a). Angles are given in degrees and bond lengths in Ångstroms.

(A color version of this figure is available in the online journal.)

& Dunning 1995). We also predicted theoretically relative yields of the reaction products under single-collision conditions by conducting Rice–Ramsperger–Kassel–Marcus (RRKM) calculations (Eyring et al. 1980; Robinson & Holbrook 1972; Steinfield et al. 1999) of energy-dependent rate constants for individual unimolecular steps and of branching ratios of different channels. The computational procedure for these calculations has been described in detail in our previous works (Zhang et al. 2010).

3. RESULTS AND DISCUSSION

3.1. Electronic Structure Calculations

Electronic structure calculations were conducted to predict relative energies of local minima, transition states, and reaction products with an accuracy of ± 8 kJ mol⁻¹ (Figure 2). These calculations suggest that the cyano radical reacts without an entrance barrier through an indirect reaction mechanism via an addition with its carbon and/or nitrogen atom to the terminal carbon–carbon double bond of the 1,3-butadiene molecule forming doublet reaction intermediates [i1] and [i5]. The initial collision complex [i1] can undergo a hydrogen atom elimination from the terminal carbon atom yielding the 1-cyano-1,3-butadiene molecule via a tight exit transition state located 14 kJ mol⁻¹ above the final products in an overall exoergic reaction (-96 kJ mol⁻¹). The computations also indicate that [i1] can isomerize yielding either the isocyano addition complex [i5] or ultimately a cyclic intermediate [i4]: a ring closure from [i1] to [i2] followed by a hydrogen shift to [i4] and a hydrogen shift in [i2] to yield [i3] followed by cyclization to [i4]. Comparing the barrier of 46 kJ mol⁻¹ ([i3]→[i4]) versus 114 kJ mol⁻¹ ([i3]→1-cyano-1,3-butadiene + H), we can conclude that isomerization to [i4] is favorable. Among these barriers, only the transition state connecting [i2] with [i4] is above the energy of

the separated reactants with 4 kJ mol⁻¹. However, within the accuracy of the calculations, we recognize that this transition state could also be slightly lower than the energy of the reactants. Note that [i5] preferentially isomerizes to [i2]; the alternative hydrogen loss pathway to form the 1-isocyano-1,3-butadiene molecule has to surmount a barrier of 13 kJ mol⁻¹. Even within the errors of our calculations (± 8 kJ mol⁻¹), we have to conclude that this barrier cannot be overcome in cold extraterrestrial environments, but only in high temperature combustion flames. Ultimately, the cyclic intermediate [i4] can eject hydrogen via a tight exit transition state located 25 kJ mol⁻¹ above the pyridine plus atomic hydrogen products in an overall exoergic reaction (-195 kJ mol⁻¹).

Finally, we attempted to apply our computations to predict the branching ratios of the formation of pyridine versus the 1-cyano-1,3-butadiene products. As it turned out, the branching ratios depend on the energies of the transition states, in particular the relative energies of the transition states connecting [i1] via [i3] to [i4] and [i1] to the 1-cyano-1,3-butadiene products. According to our RRKM calculations, using the exact energies as shown in Figure 2, only about 0.06% pyridine is predicted to be formed at a collision energy of 26.1 ± 0.9 kJ mol⁻¹; this fraction is lowered to 0.02% within the limit of 0 kJ mol⁻¹ collision energy. The accuracy of our calculations should be within 8 kJ mol⁻¹. If we decrease the critical [i1]–[i3] barrier by 8 kJ mol⁻¹, this increases the pyridine fraction to 0.2%. A more drastic variation by increasing the barrier leading to 1-cyano-1,3-butadiene and simultaneously decreasing the barrier leading to pyridine by 8 kJ mol⁻¹ yields up to 6% pyridine. So to summarize, the calculations predict that the thermodynamically less stable 1-cyano-1,3-butadiene isomer represents almost the exclusive fraction of the products formed with possibly minor contributions of less than a few percent of the pyridine molecule. Finally, it should be noted that the hydrogen abstraction channels from the C1 and C2 positions

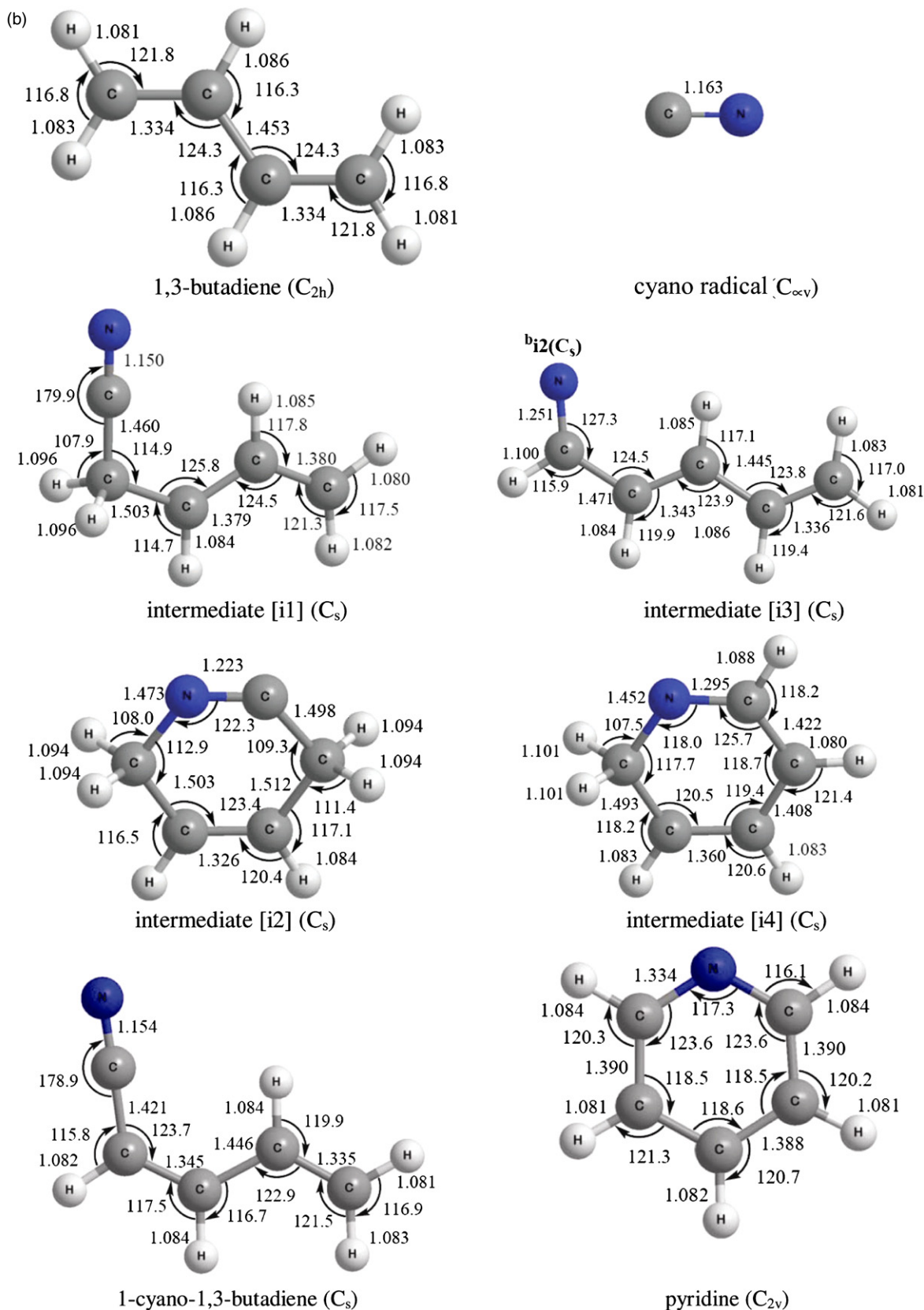


Figure 2. (Continued)

of the 1,3-butadiene molecule forming hydrogen cyanide plus two C_4H_5 radicals were calculated to have barriers of about 35 kJ mol^{-1} . Hence, these processes cannot happen in low-temperature environments such as Titan and the ISM.

3.2. Crossed Beam Experiments

The chemical dynamics studies were conducted under single collision conditions utilizing a universal crossed molecular

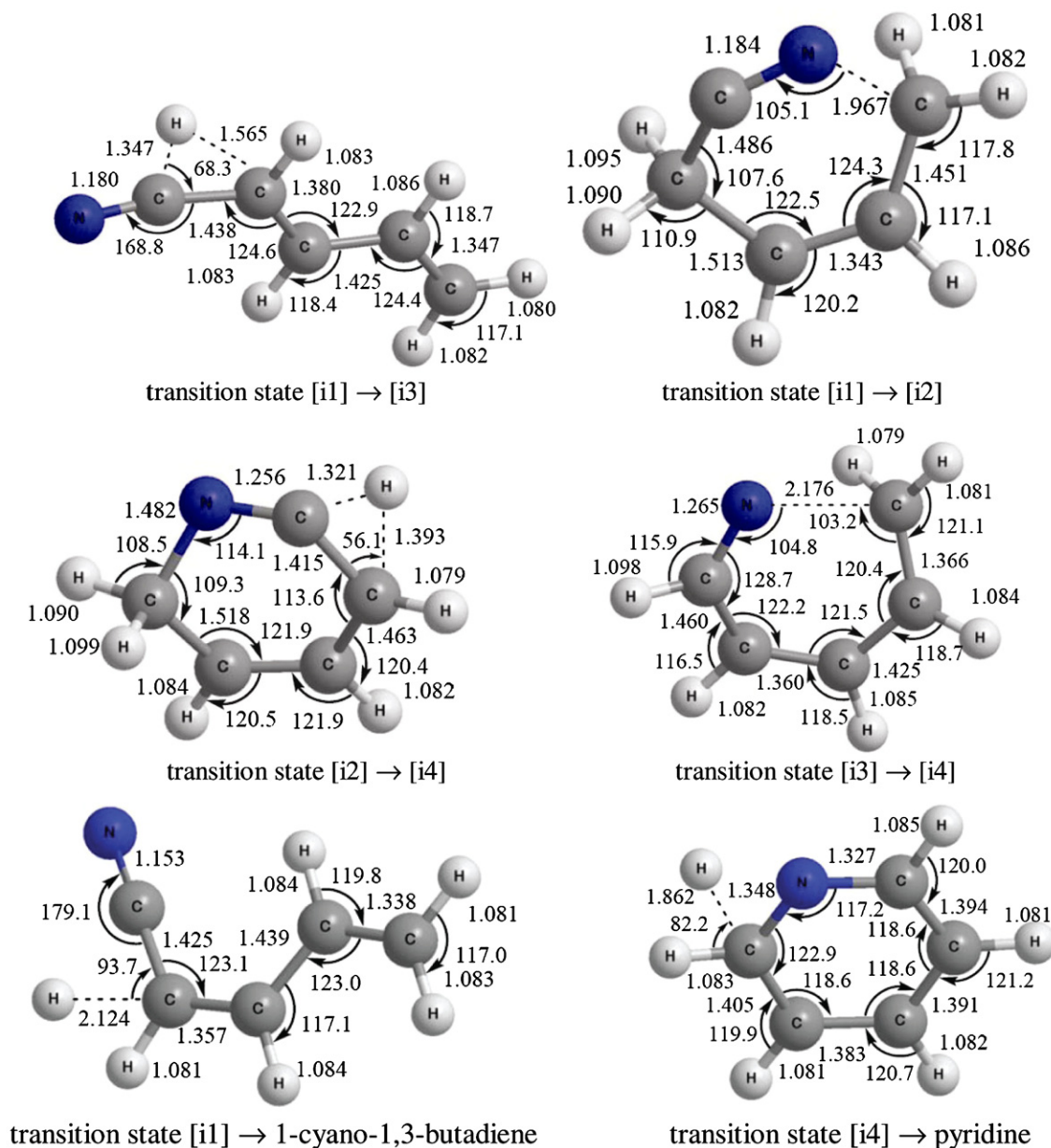


Figure 2. (Continued)

beam machine by intersecting a supersonic beam of cyano radicals ($\text{CN}(X^2\Sigma^+)$) with 1,3-butadiene ($\text{H}_2\text{CCHCHCH}_2$; X^1A_g) at a collision energy of $26.1 \pm 0.9 \text{ kJ mol}^{-1}$. TOF spectra of the ionized reaction products were recorded at various laboratory angles at mass-to-charge ratios of $m/z = 79$ ($\text{C}_5\text{H}_5\text{N}^+$) and $m/z = 78$ ($\text{C}_5\text{H}_4\text{N}^+$). A signal at $m/z = 79$ clearly indicates the formation of a molecule with the gross formula $\text{C}_5\text{H}_5\text{N}$ plus a light hydrogen atom via a single collision event (Figure 3). TOF spectra recorded at the lower mass-to-charge ratio of $m/z = 78$ showed after scaling a pattern identical to the TOFs recorded at $m/z = 79$. Therefore, a signal at $m/z = 78$ resulted from dissociative ionization of $\text{C}_5\text{H}_5\text{N}$ in the electron impact ionizer. Since the hydrogen atoms in 1,3-butadiene ($\text{H}_2\text{CCHCHCH}_2$) are chemically non-equivalent, we also conducted experiments of cyano radicals with partially deuterated 1,3-butadiene which indicated that the emitted hydrogen atom originates from the terminal (C1/C4) carbon atoms of the hydrocarbon reactant. The laboratory angular distribution of $m/z = \text{C}_5\text{H}_5\text{N}^+$ is shown

in Figure 4. This distribution is obtained by integrating the TOF spectra at different laboratory angles and scaling these spectra according to the data accumulation time. The resulting laboratory angular distribution extends more than 50° in the scattering plane. Also, the laboratory angular distribution of the heavy reaction products with the molecular formula $\text{C}_5\text{H}_5\text{N}$ is forward-backward symmetric and displays a maximum at 40° close to the CM angle of 42.3° . This indicates that the reaction dynamics are likely indirect and involve the existence of $\text{C}_5\text{H}_6\text{N}$ complex(es).

To gain meaningful information on the chemical dynamics and reaction mechanisms, it is important to transform the data from the laboratory to the CM reference frame. The corresponding CM angular and translational energy distributions are visualized in Figure 5. Here, data could be fit with a single channel with a translational energy distribution in point form. The maximum translational energy, E_{max} , corresponds to the sum of the collision energy and the reaction exoergicity. Therefore, a subtraction

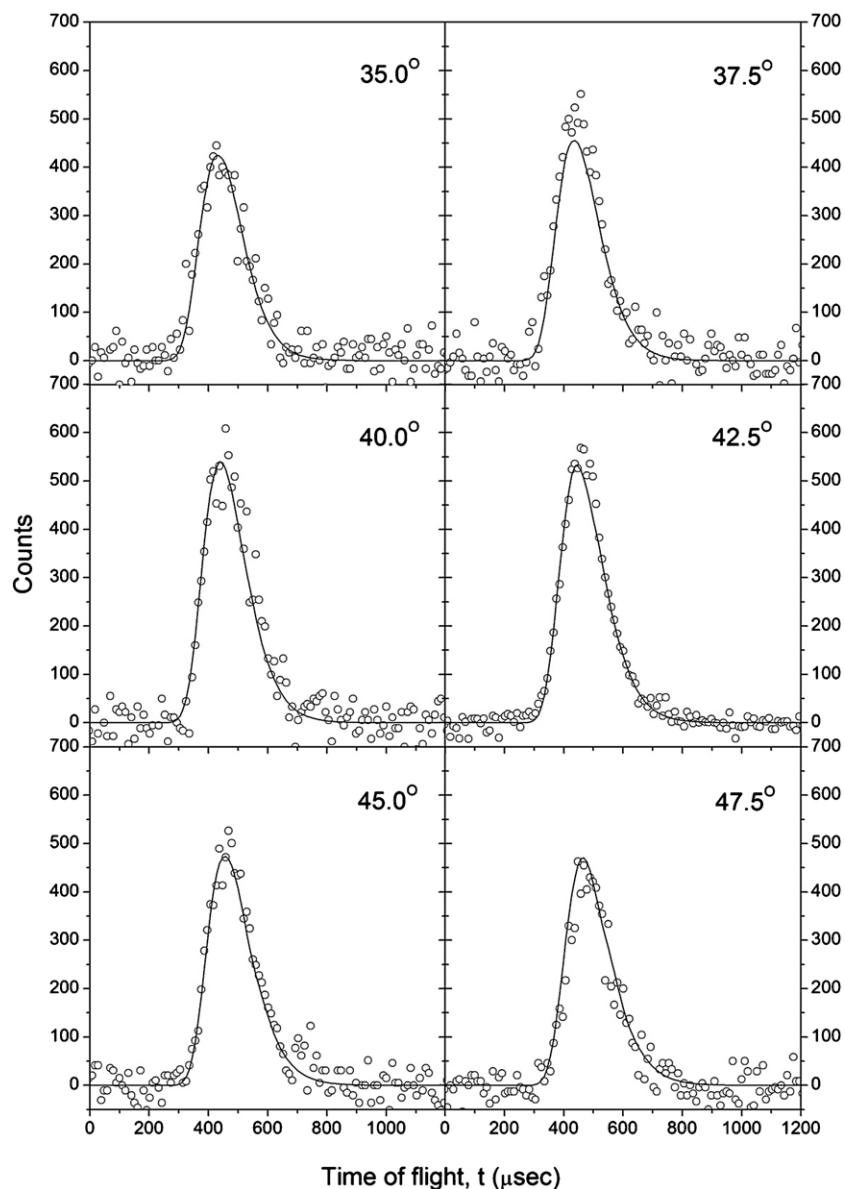


Figure 3. Time-of-flight (TOF) spectra for ions at a mass-to-charge ratio of $m/z = 79$ ($C_5H_5N^+$) of the reaction of cyano radicals with 1,3-butadiene. Circles denote experimental data; solid lines denote the calculated distributions.

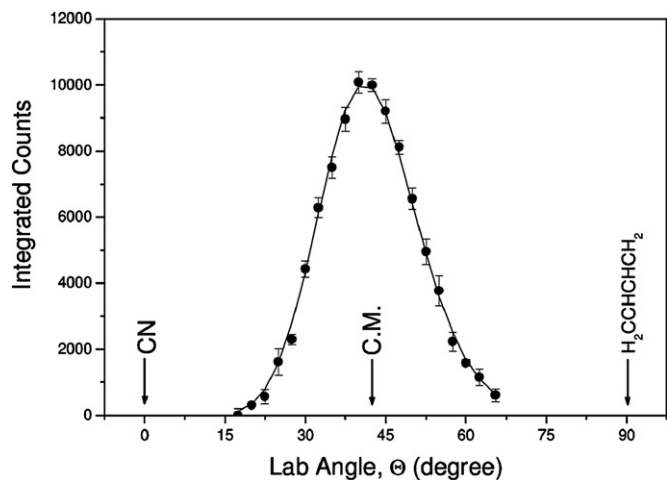


Figure 4. Laboratory angular distribution for ions at a mass-to-charge ratio of $m/z = 79$ ($C_5H_5N^+$) of the reaction of cyano radicals with 1,3-butadiene. Circles denote experimental data and solid lines denote the calculated distributions.

of the collision energy from the maximum translational energy suggests that the reactions to form the C_5H_5N isomer(s) is (are) exoergic by $189 \pm 15 \text{ kJ mol}^{-1}$; a comparison with NIST data on the reaction energies of various C_5H_5N isomers might suggest the formation of the pyridine isomer; the second most stable isomer, the 1-cyano-1,3-butadiene molecule, is about 100 kJ mol^{-1} less stable than pyridine. The formation of this isomer should be reflected in a high-energy cutoff at about 115 kJ mol^{-1} . Recall that the electronic structure calculations predict that the acyclic 1-cyano-1,3-butadiene molecule presents the dominating reaction product. Does this theoretical prediction correlate with the CM translation energy distribution derived from the experimental data? We have to admit that our cyano radical beam has a limited speed ratio, and also the fraction of vibrationally excited cyano radicals in $v = 1$ and 2 might be responsible for the “tail” of the CM translational energy distribution beyond 115 kJ mol^{-1} . In an attempt to estimate the upper limit of the pyridine fraction—if formed—we take the theoretical reaction energy of the 1-cyano-1,3-butadiene molecule plus the

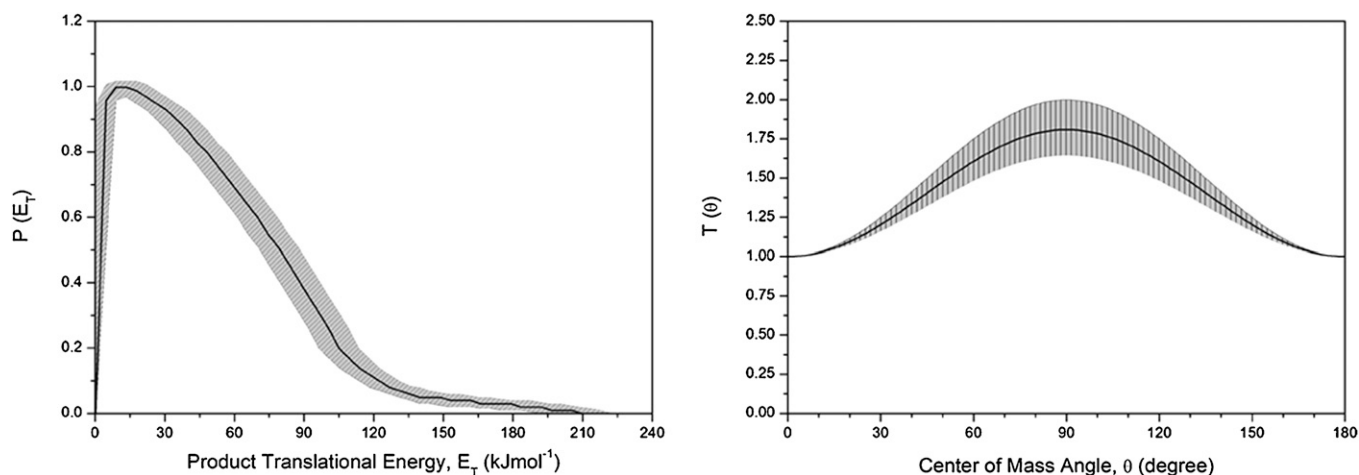


Figure 5. Center-of-mass translational energy distribution (left) and angular distribution (right) derived for the formation of $\text{C}_5\text{H}_5\text{N}$ plus atomic hydrogen in the reaction of cyano radicals with 1,3-butadiene. The shaded areas delimit the range of acceptable fits within the error limits, whereas the lines define the “best-fit” functions.

collision energy and assume all reaction products at higher energies account for pyridine. Further, upon electron impact ionization, the parent ion of the pyridine molecule is more stable than the corresponding ion of the 1-cyano-1,3-butadiene molecule. This overemphasizes the possible production of pyridine in the raw data. These corrections suggest that a maximum of 3%–6% pyridine and 94%–97% 1-cyano-1,3-butadiene are formed under our experimental conditions. However, it should be stressed that although we can be confident that based on our experiments and theoretical treatment the 1-cyano-1,3-butadiene presents the dominant product, the possible formation of pyridine has to be confirmed in future studies utilizing cyano radical beams with enhanced speed ratios; the limited speed ratio and/or vibrational energy of the cyano radicals might be an alternative reason of the “tail” in the CM translational energy distribution extending beyond 115 kJ mol^{-1} . Finally, we should indicate that the PES explains why hydrogen emission was observed only in the reaction of the cyano radical with D2–1,3-butadiene, but not in the reaction with D4–1,3-butadiene. Here, the reaction of cyano radicals with partially deuterated D2–1,3-butadiene leads to an $\text{H}_2\text{CCDCDCH}_2\text{CN}$ intermediate D2-[i1]; only an emission of a terminal hydrogen atom leads to 1-cyano-1,3-butadiene. Likewise, D2-[i1] undergoes only a hydrogen atom, but no deuterium atom migration, to D2-[i3] followed by ring closure to D2-[i4]. A hydrogen atom ejection from D2-[i4] can lead to the synthesis of D2-pyridine—if formed in minor amounts.

3.3. Kinetics Studies

The combination of the crossed beam studies with the electronic structure calculations provided crucial information on the underlying reaction dynamics on the formation of the 1-cyano-1,3-butadiene molecule under single collision conditions. However, crossed molecular beam experiments cannot provide temperature-dependent rate coefficients. These rate coefficients constitute—along with the nature of the reaction products—crucial information needed to judge if the reaction is relevant to low-temperature extraterrestrial environments. The rate coefficients are also sensitive to the absence or the presence of small barriers to reaction, which are sometimes difficult to investigate computationally. Therefore, kinetics, dynamics, and electronic structure calculations must be regarded as highly complementary. Here, the rate coefficients have been measured at several temperatures between 23 K and 200 K using a CRESU

(Cinétique de Réaction en Ecoulement Supersonique Uniforme) apparatus, originally developed by Rowe and co-workers for the study of ion–molecule reactions (Canosa et al. 2008; Rowe et al. 1984). In addition, the rate coefficients were determined at room temperature (298 K) by increasing the pressure in the main chamber up to the same pressure of the reservoir ($\sim 10 \text{ mbar}$); in this case, a subsonic flow is generated. We also performed studies of reactivity as a function of the total density. Measurements were performed at 52 K using two different nozzles functioning with argon as a buffer gas but with two different densities: $5.1 \times 10^{16} \text{ cm}^{-3}$ and $10.3 \times 10^{16} \text{ cm}^{-3}$, and at 298 K using two different pressure conditions to obtain total densities of 10^{16} cm^{-3} and $11.8 \times 10^{16} \text{ cm}^{-3}$, respectively (Table 1). In both cases, at 52 K and 298 K, rate coefficients measured were indistinguishable within the error bars. The lack of pressure dependence observed does not necessarily indicate that the reactions in question are non-associative in nature, as, given the size of the potential collision complexes, they could already be in their high pressure limits under the experimental conditions of this study. The measurements demonstrate that the variation of the rate coefficient with temperature is slight (Figure 6). The reaction remains very fast down to 23 K, the lowest temperature at which measurements were made. The slight positive temperature dependence observed over the entire range of measurements, from 23 K to 298 K, is rather unusual for a fast neutral–neutral reaction of cyano radicals with unsaturated hydrocarbons. Previous CRESU experiments involving, for instance, acetylene and ethylene suggest that these reactions have no activation energy (Sims et al. 1993). In the case of the reaction of cyano radicals with 1,3-butadiene, the temperature-dependent rate coefficients, $k(T)$, can be well represented by a simple Arrhenius expression $k(T) = (4.8 \pm 0.1) \times 10^{-10} \exp[(-77 \pm 10) \text{ J mol}^{-1}/RT] \text{ cm}^3 \text{ molecule}^{-1} \text{ s}^{-1}$ with R being the ideal gas constant and T the temperature in Kelvin. The temperature dependence of the rate constant is also very well modeled by a long-range transition state theory calculation (Georgievskii & Klippenstein 2005) which is shown as a dashed line in Figure 6, giving absolute values within 30% of the measured rate constants.

The kinetics of the cyano plus 1,3-butadiene reaction have only been studied once before by modern methods capable of correctly isolating this fast radical–molecule reaction, by Butterfield et al. (1993). They measured temperature-dependent

Table 1
Rate Coefficients Measured between 23 and 298 K for the Reaction of CN with 1,3-butadiene

T (K)	Buffer Gas	Total Density (10^{16} molecule cm^{-3})	$[\text{C}_4\text{H}_6]$ (10^{13} molecule cm^{-3})	Number of Experimental Points	Rate Coefficient, k (10^{-10} cm^3 molecule $^{-1}$ s^{-1})
23	He	4.73	0–10.91	10	3.23 ± 0.47^a
39	N_2	3.2	0–1.94	15	3.80 ± 0.57
52	Ar	10.3	0–4.26	12	3.89 ± 0.42
52	Ar	5.15	0–3.80	14	4.00 ± 0.54
83	N_2	4.88	0–3.12	11	4.33 ± 0.50
120	He	12.7	0–4.34	12	4.66 ± 0.64
200	N_2	5.57	0–17.44	13	4.34 ± 0.45
298	N_2	11.8	0–18.9	11	4.51 ± 0.50
298	N_2	1.0	0–9.47	11	4.87 ± 0.52

Notes. ^a Uncertainties (here and throughout the table) are calculated using the standard error evaluated from the second-order plot, multiplied by the appropriate Student's t factor for 95% confidence. An estimated systematic error of 10% was combined with this to yield the overall estimated uncertainty: $\sigma = \sqrt{(\sigma_{\text{stat}})^2 + (\sigma_{\text{syst}})^2}$.

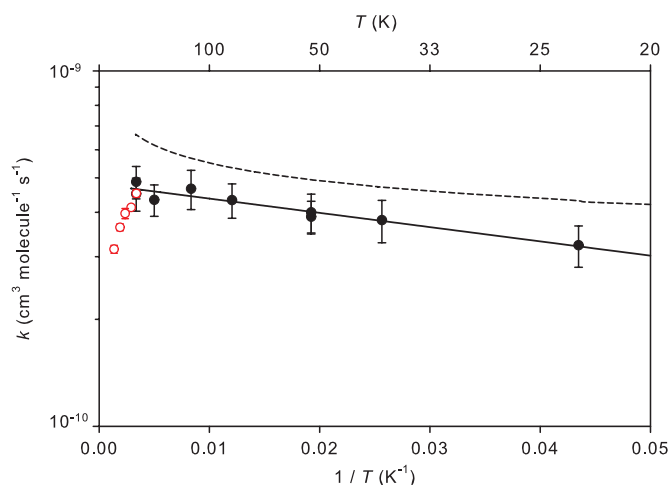


Figure 6. The filled circles (●) show the rate coefficient, k , for the reaction of cyano radicals with 1,3-butadiene plotted on a log scale vs. the inverse temperature in Kelvin $^{-1}$. The solid black line corresponds to the Arrhenius function given in the text. The open circles (○) represent the previous results of Butterfield et al. (1993). The dashed line shows the results of the long-range transition theory calculation referred to in the text.

(A color version of this figure is available in the online journal.)

rate coefficients of the following form: $k = (2.57 \pm 0.24) \times 10^{-10} \exp[(+1.41 \pm 0.28) \text{ kJ mol}^{-1}/RT] \text{ cm}^3 \text{ molecule}^{-1} \text{ s}^{-1}$ over the range 297–740 K. The rate coefficient for this reaction has never before been measured at low temperatures. The results of this study are in good agreement at room temperature with Butterfield et al., but, as can be seen from Figure 6, the very mild positive temperature dependence that we find is in marked contrast to the strong fall in the rate coefficient at higher temperatures reported by Butterfield et al. Such a significant fall at higher temperatures has also been observed by Butterfield et al. for the reaction between the cyano radical and propene, a result in disagreement with the high temperature study of Herbert et al. (1992). It is difficult, however, to comment further on these discrepancies as Butterfield et al.'s article does not, for example, specify the pressure at which these measurements were performed.

4. ASTROPHYSICAL IMPLICATIONS

Our combined dynamics, kinetics, and theoretical investigation represent a first step toward a systematic understand-

ing of how complex, nitrogen-bearing molecules may form in low-temperature environments under collision-free conditions. While the kinetics studies provided temperature-dependent rate coefficients demonstrating that even at low temperatures the overall reaction is fast, close to the gas-kinetic limit, the dynamic studies were able to identify the 1-cyano-1,3-butadiene isomer as the dominating reaction product; possible minor fractions of the aromatic pyridine isomer have to be confirmed in future studies. Under the low-temperature conditions of the atmosphere of Saturn's moon, Titan, this barrier-less and exoergic reaction could contribute to the synthesis of $\text{C}_5\text{H}_5\text{N}$ isomers—here mostly the 1-cyano-1,3-butadiene. A thorough data analysis from the Ion and Neutral Mass Spectrometer on board the *Cassini* spacecraft assigned ions monitored at $m/z = 80$ to be $\text{C}_5\text{H}_5\text{NH}^+$ (Waite et al. 2005). These ions were assumed to be formed exclusively by proton transfer to the $\text{C}_5\text{H}_5\text{N}$ neutral and a mixing ratio at 1100 km for $\text{C}_5\text{H}_5\text{N}$ of about 4×10^{-7} was retrieved.

It is interesting to compare the present findings of an (almost) exclusive formation of the acyclic 1-cyano-1,3-butadiene with the results of the isoelectronic reaction of ethynyl radicals with 1,3-butadiene (Jones et al. 2011). Here, the benzene molecule can be formed via a barrier-less, exoergic reaction with 1,3-butadiene at significant fractions of $30\% \pm 10\%$; the thermodynamically less stable hexa-1,3-dien-5-yne isomer was found to be a second isomer. A closer look at the involved PESs suggests that the intermediate analogous to [i5] in the reaction of ethynyl with 1,3-butadiene is stabilized by 282 kJ mol^{-1} with respect to the separated reactants, i.e., a potential energy well which is deeper by about 100 kJ mol^{-1} compared to [i5]. On the C_6H_7 PES, the corresponding cyclization from [i5] to [i2] and hydrogen shift to [i4] are passing barriers which are 181 and 144 kJ mol^{-1} lower than the reactants. These are located significantly lower than those calculated at -90 and $+4 \text{ kJ mol}^{-1}$ with respect to the separated reactants as found for the $\text{C}_5\text{H}_6\text{N}$ system. Also, the *relative* barriers to ring closure (85 versus 101 kJ mol^{-1}) and hydrogen migration (195 versus 174 kJ mol^{-1}) are similar for the cyano and ethynyl reactions; however, the initial formation of the energetically less favorable cyano addition product [i5] versus the ethynyl addition product formed in the C1 radical addition to 1,3-butadiene results in energetically higher transition states on the $\text{C}_5\text{H}_6\text{N}$ PES compared to the C_6H_7 PES. This effectively reduces the formation of pyridine (compared to its acyclic isomer), but still

leads to significant fractions of benzene on the C₆H₇ surface. Consequently, the substitution of a single nitrogen atom by an isoelectronic CH moiety in cases of isoelectronic cyano and ethynyl reactions are likely to be reflected in a favorable formation of benzene compared to pyridine in the ISM and in Titan's atmosphere. It remains to be seen via atmospheric modeling if this finding can be transferred to N-PAHs, which should be less abundant than their PAH counterparts if formed via neutral–neutral reactions.

It is also important to highlight that bimolecular reactions such as these are not necessarily controlled by their thermodynamics, and—as in the present case study—the thermodynamically less stable isomer may represent the (almost) exclusive product.

The experimental work was supported by the Chemistry division of the US National Science Foundation (NSF-CRC CHE-0627854). The Rennes team also gratefully acknowledges support from the European Union (RTN Network “Molecular Universe,” contract MRTN-CT-2004-512302), the Région de Bretagne and Rennes Metropole, as well as the Programme National “Physique et Chimie du Milieu Interstellaire” and the Programme National “Planétologie.” B.J.S., P.T.C., and A.H.H.C. acknowledge the National Center for High Performance Computer of Taiwan for providing computer resources.

REFERENCES

- Allamandola, L. J., Tielens, A., & Barker, J. R. 1985, *ApJ*, **290**, L25
 Allamandola, L. J., Tielens, A., & Barker, J. R. 1989, *ApJS*, **71**, 733
 Balucani, N., Asvany, O., Huang, L. C. L., et al. 2000, *ApJ*, **545**, 892
 Baronavski, A. P., & McDonald, J. R. 1977, *Chem. Phys. Lett.*, **45**, 172
 Becke, A. D. 1993, *J. Chem. Phys.*, **98**, 5648
 Belloche, A., Garrod, R. T., Müller, H. S. P., et al. 2009, *A&A*, **499**, 215
 Belloche, A., Menten, K. M., Comito, C., et al. 2008, *A&A*, **482**, 179
 Butterfield, M. T., Yu, T., & Lin, M. C. 1993, *Chem. Phys.*, **169**, 129
 Canosa, A., Goulay, F., Sims, I. R., & Rowe, B. R. 2008, in *Low Temperatures and Cold Molecules*, ed. I. W. M. Smith (Singapore: World Scientific), 55
 Cernicharo, J., Heras, A. M., Tielens, A., et al. 2001, *ApJ*, **546**, L123
 Chastaing, D., James, P. L., Sims, I. R., & Smith, I. W. M. 1998, *Faraday Discuss.*, **109**, 165
 Chin, Y. N., Kaiser, R. I., Lemme, C., & Henkel, C. 2006, in *AIP Conf. Proc.* 855, *Astrochemistry: From Laboratory Studies to Astronomical Observations*, ed. R. I. Kaiser, P. Bernath, Y. Osamura, S. Petrie, & A. M. Mebel (Melville, NY: AIP), 149
 Cook, D. J., Schlemmer, S., Balucani, N., et al. 1996, *Nature*, **380**, 227
 Des Marais, D. J., Nuth, J. A., III, Allamandola, L. J., et al. 2008, *Astrobiology*, **8**, 715
 Draine, B. T., & Li, A. 2007, *ApJ*, **657**, 810
 Entenman, E. A. 1986, PhD thesis Harvard Univ.
 Eyring, H. J., Lin, S. H., & Lin, S. M. 1980, *Basic Chemical Kinetics* (New York: Wiley)
 Frisch, M. J., Trucks, G. W., Schlegel, H. B., et al. 2004, *Gaussian 03*, Revision A.11 (Wallingford, CT: Gaussian, Inc.)
 Georgievskii, Y., & Klippenstein, S. J. 2005, *J. Chem. Phys.*, **122**, 194103
 Hahndorf, L., Lee, H. Y., Mebel, A. M., et al. 2000, *J. Chem. Phys.*, **113**, 9622
 Herbert, L., Smith, I. W. M., & Spencer-Smith, R. D. 1992, *Int. J. Chem. Kinet.*, **24**, 791
 Herbst, E., & van Dishoeck, E. F. 2009, *AR&AA*, **47**, 427
 Jones, B. M., Zhang, F. T., Kaiser, R. I., et al. 2011, *Proc. Natl Acad. Sci. USA*, **108**, 452
 Kaiser, R. I., & Balucani, N. 2001, *Acc. Chem. Res.*, **34**, 699
 Kaiser, R. I., Ting, J. W., Huang, L. C. L., et al. 1999, *Rev. Sci. Instrum.*, **70**, 4185
 Lee, C. T., Yang, W. T., & Parr, R. G. 1988, *Phys. Rev. B*, **37**, 785
 Li, A. G., & Draine, B. T. 2001, *ApJ*, **554**, 778
 Liszt, H. S., Pety, J., & Lucas, R. 2008, *A&A*, **486**, 493
 Lovas, F. J., Hollis, J. M., Remijan, A. J., & Jewell, P. R. 2006a, *ApJ*, **645**, L137
 Lovas, F. J., Remijan, A. J., Hollis, J. M., Jewell, P. R., & Snyder, L. E. 2006b, *ApJ*, **637**, L37
 Peeters, E. 2011, in *PAHs and the Universe: A Symposium to Celebrate the 25th Anniversary of the PAH Hypothesis*, ed. C. Joblin & A. G. G. M. Tielens (EAS Publication series; Toulouse: EDP Sciences), 13
 Peterson, K. A., & Dunning, T. H. 1995, *J. Phys. Chem.*, **99**, 3898
 Pople, J. A., Head-Gordon, M., & Raghavachari, K. 1987, *J. Chem. Phys.*, **87**, 5968
 Purvis, G. D., & Bartlett, R. J. 1982, *J. Chem. Phys.*, **76**, 1910
 Rhee, Y. M., Lee, T. J., Gudipati, M. S., Allamandola, L. J., & Head-Gordon, M. 2007, *Proc. Natl Acad. Sci. USA*, **104**, 5274
 Robinson, P. J., & Holbrook, K. A. 1972, *Unimolecular Reactions* (New York: Wiley)
 Rowe, B. R., Dupeyrat, G., Marquette, J. B., & Gaucherel, P. 1984, *J. Chem. Phys.*, **80**, 4915
 Salama, F., & Allamandola, L. J. 1992, *Nature*, **358**, 42
 Scuseria, G. E., Janssen, C. L., & Schaefer, H. F. 1988, *J. Chem. Phys.*, **89**, 7382
 Scuseria, G. E., & Schaefer, H. F. 1989, *J. Chem. Phys.*, **90**, 3700
 Sims, I. R., Queffelec, J. L., Defrance, A., et al. 1994, *J. Chem. Phys.*, **100**, 4229
 Sims, I. R., Queffelec, J. L., Travers, D., et al. 1993, *Chem. Phys. Lett.*, **211**, 461
 Snow, T. P., & Witt, A. N. 1995, *Science*, **270**, 1455
 Snyder, L. E., Hollis, J. M., Jewell, P. R., Lovas, F. J., & Remijan, A. 2006, *ApJ*, **647**, 412
 Soorkia, S., Taatjes, C. A., Osborn, D. L., et al. 2010, *Phys. Chem. Chem. Phys.*, **12**, 8750
 Stahl, F., Schleyer, P. V., Schaefer, H. F., & Kaiser, R. I. 2002, *Planet. Space Sci.*, **50**, 685
 Steinfield, J. I., Francisco, J. S., & Hase, W. L. 1999, *Chemical Kinetics and Dynamics* (Englewood Cliffs, NJ: Prentice Hall)
 Waite, J. H., Niemann, H., Yelle, R. V., et al. 2005, *Science*, **308**, 982
 Werner, H.-J., Knowles, P. J., Lindh, R., et al. MOLPRO, Version 2006.1, A Package of Ab Initio Programs, <http://www.molpro.net>
 Zhang, F. T., Jones, B., & Maksiyutenko, P. 2010, *J. Am. Chem. Soc.*, **132**, 2672